IEEE Access
Multidisciplinary ⋮ Rapid Review ⋮ Open Access Journal

Received January 5, 2022, accepted January 23, 2022, date of publication February 1, 2022, date of current version February 18, 2022.

Digital Object Identifier 10.1109/ACCESS.2022.3148528

Dynamic Equivalent Circuit Model to Estimate State-of-Health of Lithium-Ion Batteries

SHEHLA AMIR[1], MONEEBA GULZAR[1], MUHAMMAD O. TARAR[1], IJAZ H. NAQVI[1], (Member, IEEE), NAUMAN A. ZAFFAR[1], (Member, IEEE), AND MICHAEL G. PECHT[2], (Life Fellow, IEEE)

[1]Department of Electrical Engineering, Lahore University of Management Sciences (LUMS), Lahore 54792, Pakistan
[2]Center for Advanced Life Cycle Engineering (CALCE), University of Maryland (UMD), College Park, MD 20742, USA

Corresponding author: Ijaz H. Naqvi (ijaznaqvi@lums.edu.pk)

This work was supported in part by the Faculty Initiative Fund Grant from the Lahore University of Management Sciences under Grant FIF590-2020-EED.

ABSTRACT Lithium-ion (Li-ion) batteries have increasingly been used in diverse applications. Accurate estimation of the state of health (SOH) of the Li-ion batteries is vital for all stakeholders and critical in various applications such as electric vehicles (EVs). The electrical equivalent circuit (EEC) 2-RC model is often used to model the battery operation but has not been used to capture the degradation of battery cells over time. This paper uses the 2-RC model to capture the degradation of the Li-ion battery. The proposed model is not only time-dependent but also captures the effect of temperature on battery degradation. The proposed approach estimates the SOH accurately and is also considerably flexible for diverse cells of different chemistry. We further generalize an N-RC model approach to evaluate the SOH of the battery. We compare the proposed model (2-RC) with the 1-RC model, and through numerical results, we show that the 2-RC model outperforms 1-RC and reduces the computational cost significantly. Similarly, the 2-RC model outperforms 3-RC and higher-order circuits. We also show that the proposed approach can capture the battery dynamics better for specific smaller orders of the polynomial (associated with Arrhenius equation) when compared with the 1-RC approach with considerably reduced (up to 60%) root mean square error (RMSE). Lastly, the average testing RMSE for 2-RC is 52.4%.

INDEX TERMS Lithium-ion battery, state-of-health, equivalent circuit model, open circuit voltage.

I. INTRODUCTION

Batteries are ubiquitous in 21st century; from personal computers to residential storage units, from storage for renewable energy sources to high power electric vehicles (EVs), batteries are used as sources of energy and storage. They power medical devices, home appliances and store energy in grids. Use of batteries in EVs is getting popular as the world is facing a high rate of depletion in fossil fuels than its formation. Moreover, with the gain in popularity of EVs, smart grid technology is incorporating EVs in their models for better energy management systems [1], [2]. Therefore, to reduce failure scenarios and the need for better battery monitoring systems is rising and the need to study the degradation of battery is crucial.

Lithium-ion (Li-ion) batteries are gradually becoming the most commonly used type of battery because of their low maintenance, long lifetime, lightweight, high energy density, considerable depth of discharge, wide temperature range, low self-discharge rate, and fast charging capabilities [3]–[5]. Li-ion batteries have diverse applications and are manufactured with various storage capacities and chemistries. Some common chemistries include Lithium Cobalt Oxide (LCO), Lithium Iron Phosphate (LFP), Lithium Manganese Oxide (LMO), Lithium Nickel Cobalt Aluminum Oxide (NCA), and Lithium Nickel Manganese Cobalt Oxide (NMC). These batteries differ in their energy storage capabilities, such as energy density and power density for different applications. Li-ion technology is also entering the realm of backup power system storage because of its long cycle-life at high temperatures, high energy efficiency, and high energy utilization, even at high discharge current rates [6].

Li-ion batteries undergo a continuous degradation process [7]. The irreversible electrochemical changes, such as solid electrolyte interface (SEI) growth during repeated charging and discharging, occur in the battery [8]. Loss of

The associate editor coordinating the review of this manuscript and approving it for publication was Derek Abbott.

lithium inventory (LLI) generally results as a product of SEI growth [9]. Ageing can further be due to other reactions such as loss of active material on anode and cathode [9]. The degradation leads to reduced storage capacity and performance, and so using these batteries beyond the end of life (EOL) can lead to catastrophic results, especially in critical applications such as EVs or biomedical applications [10]. Battery management system (BMS) that monitor the health of the battery under safe operating conditions require accurate knowledge of the state of health (SOH) of battery. In order to have an accurate knowledge of the battery's degradation state, BMS execute SOH estimation algorithms [11].

SOH is generally defined as the percentage of remaining maximum capacity at a particular time compared to the nominal rated capacity at the time of manufacturing. It is defined mathematically using equation 1,

$$\mathrm{SOH}(\%) = \frac{Q_{\max}}{Q_{\mathrm{nom}}} \times 100\% \tag{1}$$

where $Q_{\max}$ is the maximum capacity of the given cycle, and Q_{nom} is the rated nominal capacity of the battery. The nominal capacity is defined as the amount of charge delivered by a fully charged battery [12].

A. LITERATURE REVIEW

Numerous methods to estimate the battery's SOH can be found in the literature. Traditionally, these methods can be divided into two categories: data-driven methods and model-based methods or a combination of both techniques.

In data-driven methods, understanding the electrochemical reactions and their modelling is not necessary and so these methods utilize only the degradation patterns present in the data using large data sets. Various methods such as Gaussian-process based Kalman filter [13]–[15], neural network (NN) [16], [17], fuzzy logic [18], [19], genetic algorithm (GA) [20], support vector machine (SVM) [21], and long short term memory (LSTM) [21], [22], and other data-driven techniques [23]–[25] have been employed for SOH estimation. These methods have high accuracy and are flexible to the changes in SOH. However, as data driven techniques are trained on particular data sets, these techniques are mostly not generalizable to unseen data [11].

The model-based approaches can be further divided into two categories; electrochemical models [26], [27], and electric equivalent circuit (EEC) models [28]–[30]. Fractional order models (FOM) are closely linked to electrochemical models. They represent the physical changes in the battery such as electrochemical reactions inside the battery [31], [32]. However, the FOM models are generally more complex compared to an integer-order model. Thus, they require more computational power and are generally slow [33]. The electrochemical model can capture the state of the electrode at a given instance. However, this approach has its drawbacks, such as requiring the computation of a large number of complex parameters and thus having a high computational cost and so would not be suitable for real-time applications such as in EVs.

Li-ion batteries are modelled as equivalent circuits comprising basic circuit elements like resistors and capacitors (RC) in the EEC model. Their time dependency can be used to model the parameters of the circuit. An EEC model based on the Thevenin equivalent circuit can be used to study the SOH of the battery as it degrades [34]. There has been extensive research on different EEC models. The two most common EEC models are the 1-RC model and the 2-RC model [11]. Bian *et al.* [29] proposed a 1-RC model lumped with an Arrhenius constant to factor in the temperature dependency of the battery degradation. The model reduced the number of parameters, but it did not factor in the battery's dynamics, such as electrochemical polarization and their transients. A 2-RC model can capture the dynamics more effectively [29]. Several techniques are utilized to estimate model parameters such as least-squares fitting [11], [35], multi-objective genetic algorithm [36], and so on. The least-squares fitting is the most straightforward technique and produces a reasonable estimate of the model parameters. Furthermore cell inconsistency analysis can be done using Thevenin equivalent circuit [37]. To limit the scope of this article we will not discuss cell consistency analysis, however, we will keep it as future work.

Transient response of the battery is the response when battery is triggered to a different state from its steady state. During the rest time, the SOH of the battery changes, and the transient response can be used to analyze the difference in the SOH of the battery after discharging [38]. However, as mentioned in [38] the accuracy achieved has an error of 3%. A model which can capture this degradation as well to enhance the accuracy of estimated SOH is a challenge.

Differential methodologies such as incremental capacity analysis (ICA) and differential voltage analysis (DVD) are used to study the degradation of the Li-ion battery [39]–[41]. These peaks shift in terms of amplitude and position with time in ICA peaks indicates degradation of the battery. The peak shifts occur due to battery ageing and failure mechanisms like loss of useful Li-ion [42], [43]. However, these approaches have a few drawbacks, such as requiring static charging and discharging over a broader range, and there are also challenges in extracting features from the IC curves [44]. With the help of the IC curve, we can find the range of values for a specific charging/discharging cycle which can help in estimating the SOH of the cycle using a small portion of the data provided [29].

B. CONTRIBUTIONS

This paper proposes a dynamic EEC model that adapts and captures the SOH dynamics over time and can reliably predict degradation in the battery's health. The model is based on the 2-RC EEC model that uses open-circuit voltage (OCV), which is the function of the state of charge (SOC). The model uses non-linear least squares curve fitting to approximate the parameter of the model which can then be used to estimate

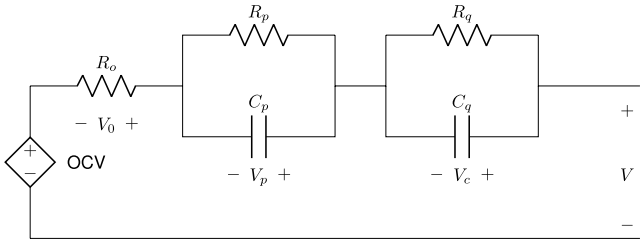

FIGURE 1. Equivalent 2-RC Model of the battery [46].

the SOH for a given cycle. To validate the model, numerical tests are performed on the Center for Advanced Life Cycle Engineering (CALCE) dataset provided by the University of Maryland (UMD) College Park and the publicly available National Aeronautics and Space Administration (NASA) Ames Research Center dataset [45].

The paper's organization is as follows; in Section II, we discuss the modeling of the Li-ion battery using resistors and capacitors. In Section III, we discuss the algorithm's development and validation to test the model. In Section IV, we evaluate the model using error metrics and compare it with the 1-RC approach. In Section IV-C we discuss a generalized N-RC model-based approach. And in Section IV-A, we discuss the voltage window and ICA peaks. In Section V, we summarize the key advantages, findings, conclusions, and future work.

II. 2-RC EQUIVALENT CIRCUIT MODEL

To model the battery and capture its dynamics, we used an EEC 2-RC model as shown in Figure 1 [46]. As the battery degrades, the rate at which the voltage drops increases. To model this trend against battery capacity, we use our 2-RC model. State of Charge (SOC) of a battery is defined as the quantity of charge stored at a given instant relative to the maximum quantity of charge that can be stored in a particular cycle. Mathematically, this can be written as

$$\text{SOC} = \frac{Q}{Q_{\max}}, \tag{2}$$

where $Q_{\max}$ is the maximum charge that can be stored which changes as the battery degrades, and Q is the charge stored at the given instant of that cycle.

A more robust way to define SOC is

$$\text{SOC} = \text{SOC}_0 + \frac{Q}{Q_{\max}}, \tag{3}$$

here we take into account the initial approximate of SOC of the cycle as SOC_0.

The battery dynamics can be expressed using basic circuit components. The Thevenin based EEC model consists of a self-discharging resistor R_0, RC parallel networks. R_p, R_q are polarization resistances where R_p captures electrochemical polarizations and R_q captures concentration polarization and C_p, C_q are polarization capacitors to capture the transients [47]. R_0 represents the electrolytic and connection resistance of the Li-ion battery as well [48]. The terminal voltage is V whereas the current I is assumed to be positive during the charging phase and negative during the discharging phase of the battery. τ_1 and τ_2 are the time constant of the cell. The OCV is a function of a given SOC and temperature. Equations (4), (5), (6), and (7) are written by applying Kirchhoff's voltage law (KVL) on Fig 1.

$$\text{OCV}(\text{SOC}, T) = V - V_p - V_q - V_o \tag{4}$$

$$V_o = IR_0 \tag{5}$$

$$V_p = V_{p,0}e^{-\frac{t}{\tau_1}} + IR_p(1 - e^{-\frac{t}{\tau_1}}) \tag{6}$$

$$V_q = V_{q,0}e^{-\frac{t}{\tau_2}} + IR_q(1 - e^{-\frac{t}{\tau_2}}) \tag{7}$$

In equation (4), V_p and V_q are the electrochemical polarization voltages, V_o is the voltage drop across the ohmic resistance. By substituting equations (5), (6), and (7) into equation (4), we get

$$\begin{aligned}\text{OCV}(\text{SOC}, T) = V &+ (IR_p - V_{p,0})e^{-\frac{t}{\tau_1}} \\ &+ (IR_q - V_{q,0})e^{-\frac{t}{\tau_2}} - I(R_o + R_p + R_q)\end{aligned} \tag{8}$$

The battery's capacity and performance degrade with temperature T [49]. The Arrhenius equation for the temperature's model is represented as [29], [33]

$$\text{OCV}(\text{SOC}, T) = e^{\frac{E}{R}(\frac{1}{T_{\text{ref}}} - \frac{1}{T})} \sum_{k=0}^{m} a_{k,\text{ref}}\text{SOC}^k, \tag{9}$$

where $a_{k,\text{ref}}$ are polynomial coefficients, E is the activation energy, T_{ref} is temperature constant and R is the energy gas constant.

Since the OCV of a battery depends on the SOC and temperature, we combine equations (8) and (9). The combined model of OCV is written as

$$\begin{aligned}V = e^{\frac{E}{R}(\frac{1}{T_{\text{ref}}} - \frac{1}{T})} &\sum_{k=0}^{m} a_{k,\text{ref}}(\text{SOC}_0 + \frac{Q}{Q_{\max}})^k \\ &-(IR_p - V_{p,0})e^{-\frac{t}{\tau_1}} \\ &-(IR_q - V_{q,0})e^{-\frac{t}{\tau_2}} + I(R_o + R_p + R_q).\end{aligned} \tag{10}$$

Here SOC_0 is the value of SOC at $t = 0$. The simplified version of the final expression can be written as

$$V = c_0 \sum_{k=1}^{m} a_{k,\text{ref}}(\text{SOC}_0 + \frac{Q}{Q_{\max}})^k + c_1 e^{p_1 Q} + c_2 e^{p_2 Q} + r, \tag{11}$$

where p_1, p_2, c_0, c_1, c_2, and r are constants for a given cycle. The mapping of coefficients is shown in Table 1.

III. MODEL TRAINING METHODOLOGY

To obtain an estimate of SOH, we use equation (11) to compute Q_{max} which will then be substituted in equation (1). The algorithm to approximate SOH has been summarized in Fig 2. The model assumes that the coefficients $c_0, c_1, c_2, p_1,$ and p_2 are constant for constant current charge/discharge cycle as

TABLE 1. Mapping of equation 11 coefficients.

Coefficient	Mapping
p_1	$-\frac{1}{I*\tau_1}$
p_2	$-\frac{1}{I*\tau_2}$
c_1	$-IR_p + V_{p,0}$
c_2	$-IR_q + V_{q,0}$
r	$I(R_o + R_p + R_q)$

we are using the V-Q profile of one cycle. The coefficients capture the trend and shape of the curve, which is why they are kept constant for one cycle. The parameters for $a_{k,kref}$ need to be computed once for the initial cycle. As these constants capture the general shape of the VQ profile. These parameters then remain constant for the remaining cycles. Afterward, only c_0, c_1, c_2, p_1, p_2, SOC, and Q_{max} are required to compute the SOH. The last cycle is defined by the user as the cycle till which we want to estimate the SOH of battery.

In this type of modeling, a constraint has to be placed on c_0 such that $c_0 \in [0.5, 1.5]$ [29]. The results also validate this restriction on c_0, as model accuracy decreases outside this range. Likewise, $Q_{max} \in [Q_{end}, Q_0]$, where Q_0 is the maximum discharge capacity of the cycle, and Q_{end} is the end capacity of the given charge/discharge cycle.

We train on the initial cycle to compute the value of $a_{1,ref}, \ldots, a_{k,ref}$. During the initial cycle, we do a 70-30 train-test split. We randomize the data for the initial cycle to avoid over-fitting. This creates a limitation, however, as the accuracy varies according to randomization. To overcome this limitation, we repeat the cycle for many iterations and average out the final value. Moreover, we utilize the ICA curve to check the fitting of the parameters. We compare the ICA curve we obtain from the estimated parameters with the original ICA curve. If the error between the two curves is low we conclude that the fitting for the first cycle is accurate and we can use the values of $a_{1,ref}, \ldots, a_{k,ref}$ obtained for the rest of the cycles. The evolution of Q_{max} is computed for every cycle by fitting equation (11) to the V-Q profile for the given cycle. The value obtained is then used to compute SOH from equation (1).

The proposed 2-RC model is compared with the 1-RC model proposed in [29]. For the 1-RC model, equation (11) reduces to

$$V = c_0 \sum_{k=1}^{m} a_{k,\text{ref}}(\text{SOC}_0 + \frac{Q}{Q_{\text{nom}}})^k + c_1 e^{p_1 Q} + r. \quad (12)$$

The same algorithm is shown in Fig 2 is used for both the 1-RC model and the 2-RC model. The RMSE for both models are compared for different values of m where m is the polynomial degree.

IV. VALIDATION AND EVALUATION

We evaluated our algorithm on the UMD CALCE dataset, and NASA Ames Research Center dataset. We performed our simulations in MATLAB using the optimization toolbox. The evaluation criteria and the results are discussed below.

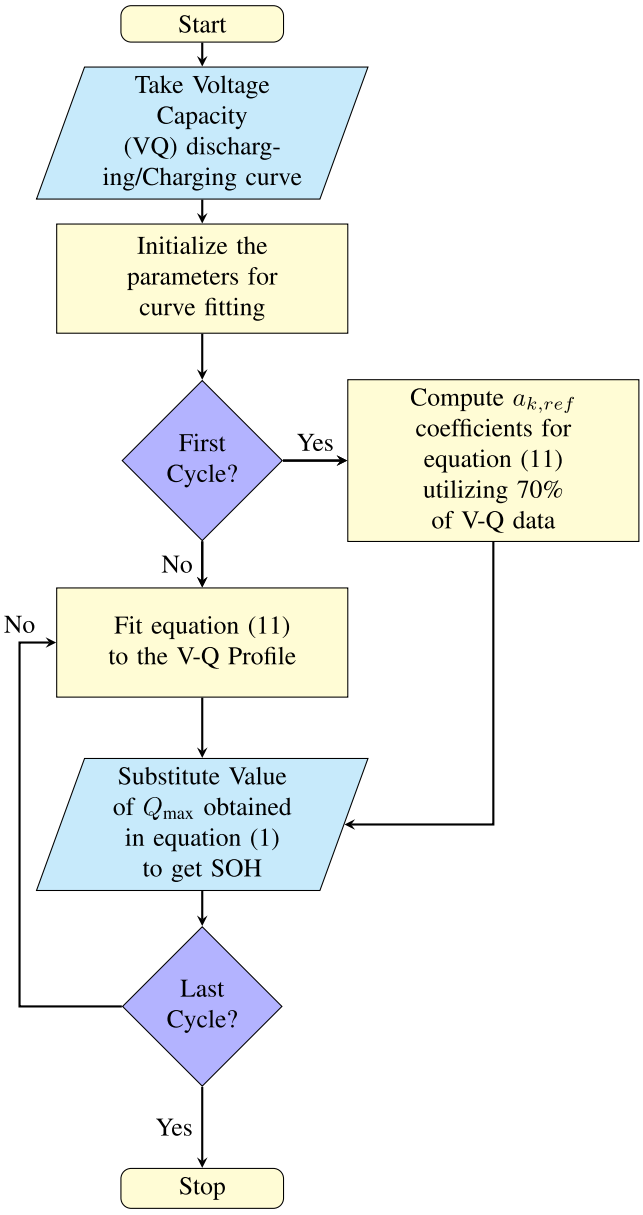

FIGURE 2. The Flow chart summarized our methodology to approximate of SOH using our model.We fit the equation 11 to the V-Q profile. We get an a value for the charge Q_{max} which is then used to compute SOH from equation 1.

A. EVALUATION METRICS

The SOH is computed utilizing the algorithm explained in Fig 2. The estimated SOH is compared with the ground truth provided in the dataset. We then calculate the RMSE defined as

$$\text{RMSE}_{\text{SOH}} = \sqrt{\frac{\sum_N (\hat{\text{SOH}} - \text{SOH})^2}{N}}, \quad (13)$$

where $\hat{SOH}$ is the predicted value of SOH for the given cycle, SOH is the ground truth, and N is the total number of cycles for a given test dataset. As explained in Section III, the V-Q data for the first cycle is randomized such that values of voltage measured are randomly indexed in the array. We compute the SOH for a different number of iterations and compute an average RMSE of SOH.

Moreover, to further prove the superiority we make use of bayesian information criterion (BIC). BIC is generally used to determine the best model given a certain dataset as it penalizes the model which has too many fitting parameters. BIC is defined as [50]

$$\text{BIC} = Dln(\sigma^2) + (k+1)ln(D) \tag{14}$$

where D is the size of the dataset, k is the order of model defined as

$$k = n + m + 1 \tag{15}$$

n is the integer order of RC pair (e.g 1,2,....) and σ is defined as

$$\sigma^2 = \frac{1}{D-k-1}\sum_{i=1}^{D}(\text{SOH}_m - \text{SOH}_e)^2 \tag{16}$$

We set D as the number of cycles present in the dataset that we are estimating on. A lower BIC score indicates that a certain model is superior.

B. RESULTS

In this section, we present the results with two different datasets: the UMD CALCE dataset and the NASA Ames dataset. The validation of the proposed scheme is done with two different datasets to show the generalizability of the proposed methodology.

1) CALCE DATASET

The CALCE dataset contains degradation data of different pouch cell batteries under 20+ test conditions with six different vendors. The cycling dataset has a constant current (CC) and constant voltage (CV) charging profile, and a CC discharging profile. Conditions such as temperature and C-rate were changed for different tests. There were two broad types of tests: cycling tests, and interval tests. In the cycling tests, only a 10 minutes rest period was used before starting the next cycle, whereas, in the interval testing, rest periods of 12 hours and 24 hours were used after each cycle. Table 2 summarizes the test conditions of the CALCE dataset.

To evaluate the proposed algorithm, we used vendor-4 test datasets. The batteries were exposed to different test conditions where discharging C-rate, rest time, and the temperature was varied. The discharging C-rate varied from 0.5C to 1.5C. The temperature varied from 25° Celsius to 55° Celsius, and rest time varied from 10 minutes to 24 hours. The cells were all charged until a cut-off voltage of 4.40 V, and the current at the CC stage was 2.25 A. During the discharging phase, the cut-off voltage of these cells was 3.0 V. Fig 3 shows

TABLE 2. UMD CALCE dataset test conditions used in this paper.

Vendor	Test No.	Temperature	C-rate	Rest Time
2	3	25	1.5	10 min
2	5	35	1.0	10 min
2	8	45	1.0	10 min
2	9	45	1.5	10 min
2	12	25	0.5	24 hr
2	15	45	0.5	12 hr
2	21	55	0.5	12 hr
4	1	25	0.5	10 min
4	3	25	1.5	10 min
4	4	35	0.5	10 min
4	5	35	1.0	10 min
4	6	35	1.5	10 min

the discharging V-Q curves for Test 1 (25° Celsius and 0.5C discharge rate). In Fig. 3, it is clear that as the battery ages, the discharging profile changes. The proposed algorithm is applied to the dataset for different polynomial orders for both 1-RC and 2-RC. We compare the results for both EEC models. The result demonstrates that for certain smaller values of m, i.e. $m = 5, 6, 7, 8$ the 2-RC model outperforms the 1-RC model. Fig. 4 compares the RMSE for different values of m, and for $m = 6, 7, 8$ the 2-RC model can better estimate the SOH. After that, for a higher value of m, we see overfitting, and the RMSE increases. The overfitting occurs due to an increase in the order of polynomials which closely follows the trend of the initial cycle for $a_{k,ref}$. However, these computed values then do not capture the trend in later cycles. Moreover, a lower value of m saves computational power and time compared to higher-order polynomials.

The proposed methodology is validated over multiple tests with different test conditions on the CALCE vendor-4 dataset. Tests 1, 3, 4, 5, and 6 are used to generate these results. In Fig. 6 where the RMSE is computed for multiple tests (1, 3, 4, 5, and 6) and averaged out. In Table 2, note that the conditions are different for different tests; for tests 1 and 3, the temperature is 25° Celsius, the discharge rates are 0.5C and 1.5C, respectively, and the rest time is 10 minutes. For tests 4, 5, and 6, the temperature is 35° Celsius, the discharge rates are 0.5C, 1C, and 1.5C, respectively, and the rest time is 10 minutes. Again we see that $m = 7$ is optimal even when averaged over multiple tests of variable test conditions. To demonstrate how closely does the model fits the ground truth, Fig 7 shows the estimated and measured SOH using the optimal value of $m = 7$ for tests 1 and 4. It is evident that measured and estimated SOHs are in close conformity. The RMSE for test 1 is 0.0535 and for test 4 is 0.0722. For 1-RC, the optimal value of m is 11 or higher, where the error is minimum. However, when we compare the time for the algorithm to run for 1-RC ($m = 11$) and 2-RC ($m = 7$), the 1-RC model requires approximately 6 seconds more in total, which get significant for large datasets.

To further validate we make use of BIC as defined in equation 14. We compute results up till 5-RC models to verify the superiority of our model and the result is shown

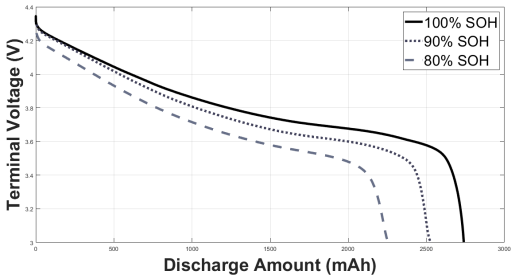

FIGURE 3. V-Q curves for all cycles for UMD Test dataset. As shown in the figure the slope of the curve decreases as SOH decreases.

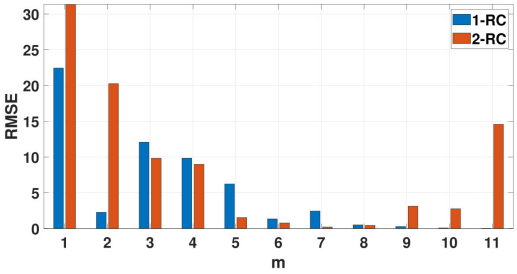

FIGURE 4. RMSE for UMD Vendor 4 Test 1 dataset. For certain smaller values of m (i.e. $m = 5, 6, 7, 8$), the 2-RC model outperforms the 1-RC EEC model.

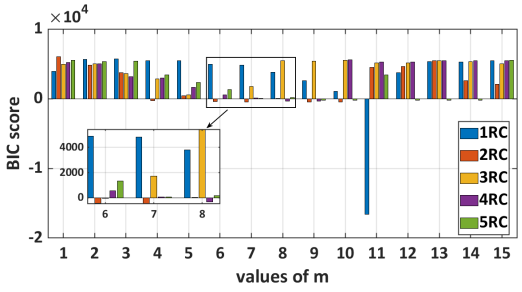

FIGURE 5. BIC score of each RC model. We computed our score for UMD vendor 2 datasets. The lowest BIC score of 2-RC model is at m = 7 where the value is −481 and for 1-RC model is at m = 11.

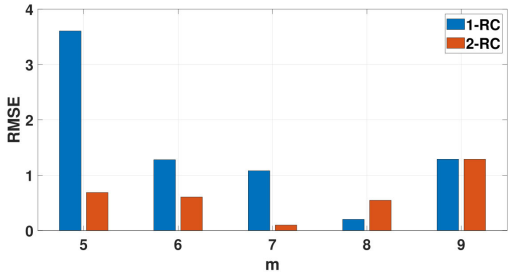

FIGURE 6. Average RMSE for Tests 1, 3, 4, 5, and 6 of UMD Vendor 4 Test dataset.

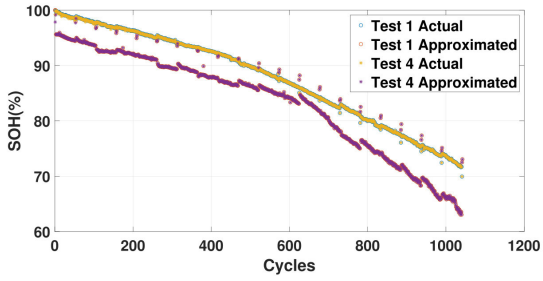

FIGURE 7. SOH approximation for Test 1 and Test 4 of UMD dataset.

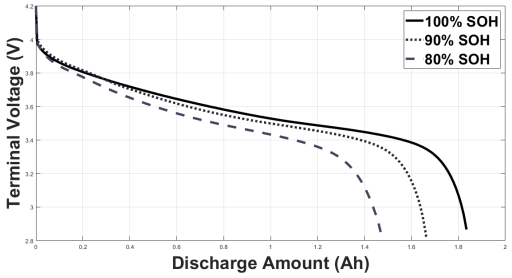

FIGURE 8. V-Q discharging profile for B0005 cell.

in figure 5. The results verify our claim that the 2-RC model performs best at $m = 7$.

2) NASA AMES DATASET

To show the generalizability of the proposed methodology, we test our algorithm on a publicly available dataset from the NASA Ames Research Center [45]. The dataset is generated from NCA cells with a nominal capacity of 2 Ah. In this paper, we utilized cells numbered B0005, B0006, B0007, and B0018. The cycling dataset has a CC and CV charging profile and a CC discharging profile. The cells are all charged until a maximum cut-off voltage of 4.2 V, and the current at the CC stage is 1.5 A. During the CV stage, the cut-off current is 20 mA. However, during the discharging phase, the cut-off voltages of these cells are 2.7, 2.5, 2.2, and 2.5 V, respectively.

To test our algorithm, we use the discharging V-Q profiles shown in Fig. 8 which are similar to the V-Q profiles of the CALCE dataset. We apply the same algorithm described in Section III. Again, we repeat our algorithm for different values of m and evaluate the results for the 1-RC and 2-RC models illustrated in Fig. 9. For 2-RC at $m = 5$, the RMSE is minimum. The RMSE stays low for a few higher values of m before it starts to increase again. In the 1-RC model, the RMSE continues to decrease for higher values of m and even performs better than the 2-RC model for $m \geq 8$, giving a better estimate of the SOH of the battery at the expense of higher computational cost. Just as observed in the CALCE dataset, the 1-RC model consumes more time than the 2-RC model (approximately 1.5 seconds). Although it looks minimal, that is due to fewer cycles (138/139) in the NASA Ames dataset. For any dataset with a higher number of cycles, the difference will become higher, an observation consistent with the fact that for the CALCE dataset, the difference was around 6 seconds for 1045 cycles. For the 2-RC model, Fig. 10 shows the SOH estimation as a function of cycles with an optimal value of $m = 5$ for the three batteries in the NASA Ames dataset. Again, the measured and the estimated SOH

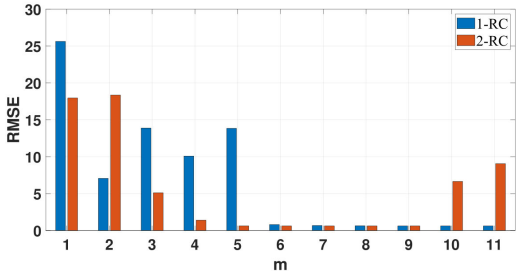

FIGURE 9. Average RMSE for different values of *m* for B0005, B0006, B0007, and B0018.

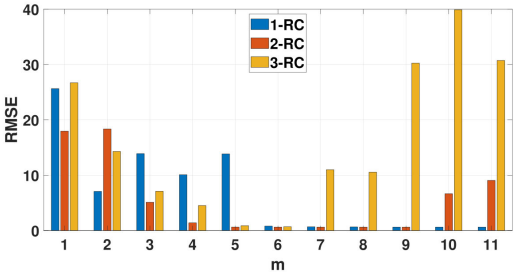

FIGURE 11. Comparison of average RMSE values of different *m* for NASA dataset (B0005, B0006, B0007, and B0018).

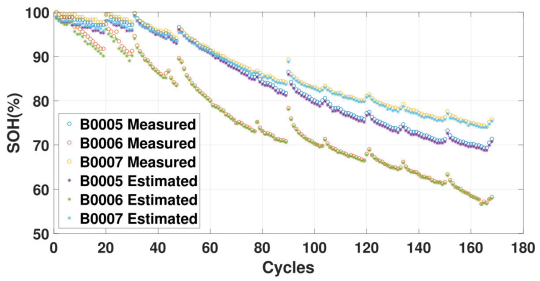

FIGURE 10. SOH Approximation for B0005, B0006, and B0007 cells.

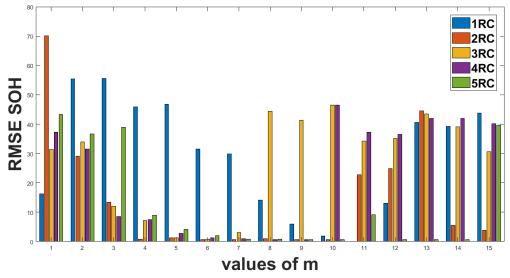

FIGURE 12. RMSE of N-RC model where N is carried from 1 to 5 for different values of the order of the polynomial (m).

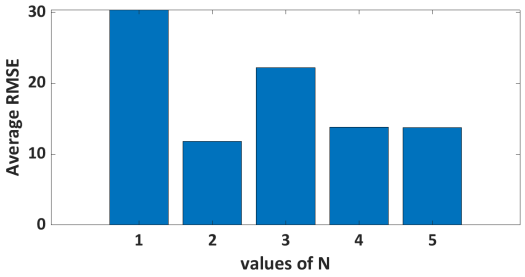

FIGURE 13. Average RMSE of N-RC model averaged over m (m varied from 1 to 10).

are in solid agreement with each other. The RMSE for SOH estimated for B0005, B0006 and B0007 is 0.7960, 0.5884, and 0.8005, respectively.

C. 3-RC AND N-RC MODEL

During the rest time, the SOH of the battery changes, and transient response can be used to analyze the difference in the SOH of the battery after discharging [38]. It can be assumed that the transient response can be expressed better using an additional RC parallel network. It might be assumed that increasing the RC network in the model will increase the model's accuracy. In this subsection, we introduce the Thevenin 3-RC EEC model. The addition of an RC parallel network adds a new exponential term and a constant term. Moreover, this approach can be extended to an N-RC model where N represents the number of parallel RC networks. Generalized N-RC equation can be written as

$$V = A\sum_{k=0}^{m} a_{k,\mathrm{ref}}(\mathrm{SOC}_0 + \frac{Q}{Q_{\mathrm{nom}}})^k + \sum_{n=1}^{N} c_n e^{P_n Q} + B, \quad (17)$$

where, $A = e^{\frac{E}{R}(\frac{1}{T_{\mathrm{ref}}} - \frac{1}{T})}$, $c_n = -(IR_n - V_{n,0})$, $P_n = -\frac{1}{I\tau_n}$, and $B = I(\sum_{n=0}^{N} R_n)$.

We repeat the same procedure explained in Sections III and IV for N = 3 for NASA dataset and N = 5 for UMD dataset to estimate the SOH of the battery. The RMSE with different order of RC models is compared in Fig. 11 and Fig. 12. The RMSE is higher for the 3-RC model compared to both 1-RC and 2-RC as shown in 13. From $m = 6$ onwards the 3-RC model overfits.

The assumption that by adding an exponential term, the model will capture the transient response better than 2-RC [51] is not valid in this case. It looks like N > 2 overfits the data, and the RMSE increases. Moreover, the datasets (both CALCE and NASA) do not have a sampling interval short enough to capture higher-order transients. Therefore, going beyond N = 2 does not provide a good fit and increases the computational complexity. However, the N-RC model is flexible, and different values of N can be used depending on the dataset and its sampling intervals. Thus, for CALCE and NASA Ames datasets, the 2-RC model suffices to estimate the SOH of Li-ion batteries.

D. VALIDATION OF 2-RC MODEL

To further evaluate our model and test whether it can predict the SOH of a battery in general, we validate the model using the CALCE vendor-2 dataset. In the vendor-2 dataset, we have three samples for one test, and all are tested under similar conditions (see Table 2). We compute coefficients

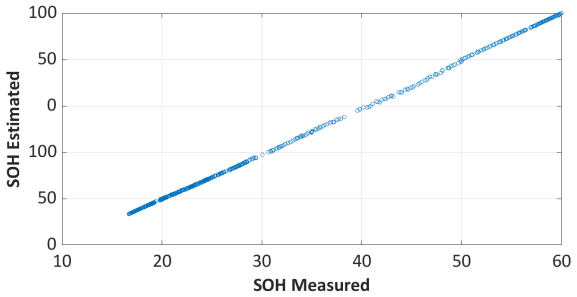

FIGURE 14. 2-RC testing on Vendor 2 Test 9 Sample 2.

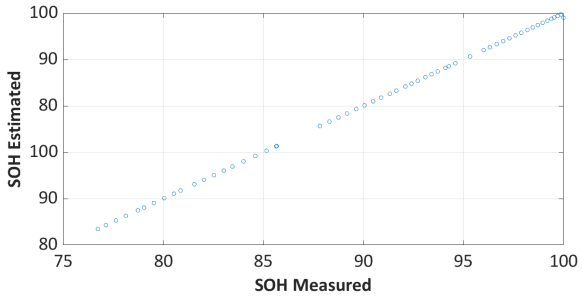

FIGURE 15. 2-RC testing on Vendor 2 Test 21 Sample 3.

TABLE 3. RMSE values for different test samples after testing.

Test 3	Test 5	Test 8	Test 9	Test 12	Test 15	Test 21
0.106	0.567	1.90	0.746	0.248	0.0385	0.0658

for the first sample and use the computed coefficients to predict the SOH for different cycles for the second and third samples. The results are shown in Fig. 14 and Fig. 15 and are summarized for selected tests in Table 3.

V. CONCLUSION

In this paper, a dynamic model based on a Thevenin EEC (2-RC) lumped with the Arrhenius equation is used to estimate the SOH. Using a simple model, we also capture the temperature's effect on the degradation of battery degradation. In this model, the OCV is expressed as a polynomial function of SOC. Thereafter, by using non-linear least squares curve fitting, we can compute the SOH for a given cycle. The results show that the 2-RC model outperforms the 1-RC model and estimates the measured SOH with considerably lower RMSE. Moreover, the 2-RC model requires a lower order of the polynomial, as compared to the 1-RC model, to approximate the SOH. This reduces the algorithm's time complexity and computational power as the number of unknowns to be determined is reduced.

Initially, it was assumed that increasing the order of the RC network in the model will increase the model's accuracy. However, the results presented in this paper show that the Thevenin 2RC EEC model achieves the lowest root mean squared error (RMSE). Adding an RC parallel network to the 1RC model adds a new exponential term and a constant term. This is represented in equation (12). Based on table 3 the average testing RMSE for 2-RC is 52.4%. Lastly, we believe that our model will work on the dynamic dataset. We plan to include analysis of dynamic dataset in our future work.

It is essential to determine the correct order of the polynomial to choose the right value of m. We show that higher values of m overfits the data and the RMSE starts increasing. The generalizability of the proposed methodology is shown by validating the model over two different data sets having different types of batteries. The results show that the 2-RC model outperforms 1-RC and N-RC models for $N > 2$.

ACKNOWLEDGMENT

The authors would also like to thank the more than 150 companies and organizations that support research activities at the Center for Advanced Life Cycle Engineering (CALCE) at the University of Maryland annually, as well as the Center for Advances in Reliability and Safety (CAIRS) of Hong Kong.

REFERENCES

[1] F. Kennel, D. Gorges, and S. Liu, "Energy management for smart grids with electric vehicles based on hierarchical MPC," *IEEE Trans. Ind. Informat.*, vol. 9, no. 3, pp. 1528–1537, Aug. 2013.
[2] L. Zhang, X. Hu, Z. Wang, J. Ruan, C. Ma, Z. Song, D. G. Dorrell, and M. G. Pecht, "Hybrid electrochemical energy storage systems: An overview for smart grid and electrified vehicle applications," *Renew. Sustain. Energy Rev.*, vol. 139, Apr. 2021, Art. no. 110581.
[3] *Is Lithium-Ion the Ideal Battery?* Accessed: Oct. 2021. [Online]. Available: https://batteryuniversity.com/article/is-lithium-ion-the-ideal-battery
[4] S. Rashidi, J. A. Esfahani, and F. Hormozi, "Classifications of porous materials for energy applications," in *Reference Module in Materials Science and Materials Engineering*. Amsterdam, The Netherlands: Elsevier, 2020.
[5] M. Kotobuki, H. Munakata, and K. Kanamura, "Chapter 4.2—All-solid-state Li battery for future energy technology," in *Handbook of Advanced Ceramics*, 2nd ed. S. Somiya, Ed. Oxford, U.K.: Academic, 2013, pp. 343–351.
[6] A. Stan, M. Swierczynski, D. Stroe, R. Teodorescu, S. J. Andreasen, and K. and Moth, "A comparative study of lithium ion to lead acid batteries for use in ups applications," in *Proc. IEEE 36th Int. Telecommun. Energy Conf. (INTELEC)*, Sep. 2014, pp. 1–8, doi: 10.1109/INTLEC.2014.6972152.
[7] X. Tang, C. Zou, K. Yao, G. Chen, B. Liu, Z. He, and F. Gao, "A fast estimation algorithm for lithium-ion battery state of health," *J. Power Sources*, vol. 396, pp. 453–458, Aug. 2018.
[8] S. J. An, J. Li, C. Daniel, D. Mohanty, S. Nagpure, and D. L. Wood, "The state of understanding of the lithium-ion-battery graphite solid electrolyte interphase (SEI) and its relationship to formation cycling," *Carbon*, vol. 105, pp. 52–76, Aug. 2016.
[9] C. R. Birkl, M. R. Roberts, E. McTurk, P. G. Bruce, and D. A. Howey, "Degradation diagnostics for lithium ion cells," *J. Power Sources*, vol. 341, pp. 373–386, Feb. 2017.
[10] M. R. Palacín and A. D. Guibert. *Why do Batteries Fail?*. (Feb. 2016). [Online]. Available: https://science.sciencemag.org/content/351/6273/1253292
[11] Y. Wang, J. Tian, Z. Sun, L. Wang, R. Xu, M. Li, and Z. Chen, "A comprehensive review of battery modeling and state estimation approaches for advanced battery management systems," *Renew. Sustain. Energy Rev.*, vol. 131, Oct. 2020, Art. no. 110015.
[12] H. Wenzl, "Batteries | capacity," in *Encyclopedia of Electrochemical Power Sources*, J. Garche, Ed. Amsterdam, The Netherlands: Elsevier, 2009, pp. 395–400.
[13] Y. Bi and S.-Y. Choe, "An adaptive sigma-point Kalman filter with state equality constraints for online state-of-charge estimation of a Li(NiMnCo)O_2/carbon battery using a reduced-order electrochemical model," *Appl. Energy*, vol. 258, Jan. 2020, Art. no. 113925.
[14] Z. Chen, L. Yang, X. Zhao, Y. Wang, and Z. He, "Online state of charge estimation of Li-ion battery based on an improved unscented Kalman filter approach," *Appl. Math. Model.*, vol. 70, pp. 532–544, Jun. 2019.

[15] Z. B. Wei, J. Y. Zhao, D. X. Ji, and K. J. Tseng, "A multi-timescale estimator for battery state of charge and capacity dual estimation based on an online identified model," *Appl. Energy*, vol. 204, pp. 1264–1274, Oct. 2017.

[16] E. Chemali, P. J. Kollmeyer, M. Preindl, and A. Emadi, "State-of-charge estimation of Li-ion batteries using deep neural networks: A machine learning approach," *J. Power Sources*, vol. 400, pp. 242–255, Oct. 2018.

[17] M. S. H. Lipu, M. A. Hannan, A. Hussain, and M. H. M. Saad, "Optimal BP neural network algorithm for state of charge estimation of lithium-ion battery using PSO with PCA feature selection," *J. Renew. Sustain. Energy*, vol. 9, no. 6, Nov. 2017, Art. no. 064102, doi: 10.1063/1.5008491.

[18] W. Pan, Q. Chen, M. Zhu, J. Tang, and J. Wang, "A data-driven fuzzy information granulation approach for battery state of health forecasting," *J. Power Sources*, vol. 475, Nov. 2020, Art. no. 228716.

[19] C. Burgos, D. Saez, M. E. Orchard, and R. Cardenas, "Fuzzy modelling for the state-of-charge estimation of lead-acid batteries," *J. Power Sources*, vol. 274, pp. 355–366, Jan. 2015.

[20] L. Chen, Z. Wang, Z. Lu, J. Li, B. Ji, H. Wei, and H. Pan, "A novel state-of-charge estimation method of lithium-ion batteries combining the grey model and genetic algorithms," *IEEE Trans. Power Electron.*, vol. 33, no. 10, pp. 8797–8807, Oct. 2018.

[21] Y. Deng, H. Ying, J. E, H. Zhu, K. Wei, J. Chen, F. Zhang, and G. Liao, "Feature parameter extraction and intelligent estimation of the state-of-health of lithium-ion batteries," *Energy*, vol. 176, pp. 91–102, Jun. 2019.

[22] Y. Fan, F. Xiao, C. Li, G. Yang, and X. Tang, "A novel deep learning framework for state of health estimation of lithium-ion battery," *J. Energy Storage*, vol. 32, Dec. 2020, Art. no. 101741.

[23] S. S. Sheikh, M. Anjum, M. A. Khan, S. A. Hassan, H. A. Khalid, A. Gastli, and L. Ben-Brahim, "A battery health monitoring method using machine learning: A data-driven approach," *Energies*, vol. 13, no. 14, p. 3658, Jul. 2020.

[24] K. A. Severson, P. M. Attia, N. Jin, N. Perkins, B. Jiang, Z. Yang, M. H. Chen, M. Aykol, P. K. Herring, D. Fraggedakis, M. Z. Bazant, S. J. Harris, W. C. Chueh, and R. D. Braatz, "Data-driven prediction of battery cycle life before capacity degradation," *Nature Energy*, vol. 4, no. 5, pp. 383–391, Mar. 2019, doi: 10.1038/s41560-019-0356-8.

[25] M. Dubarry and D. Beck, "Big data training data for artificial intelligence-based Li-ion diagnosis and prognosis," *J. Power Sources*, vol. 479, Dec. 2020, Art. no. 228806.

[26] J.-Y. Kim, J.-Y. Kim, M.-K. Kim, and J.-W. Byeon, "Health monitoring of mechanically fatigued flexible lithium ion battery by electrochemical impedance spectroscopy," *Microelectron. Rel.*, vol. 114, Nov. 2020, Art. no. 113818.

[27] K. K. Sadabadi, X. Jin, and G. Rizzoni, "Prediction of remaining useful life for a composite electrode lithium ion battery cell using an electrochemical model to estimate the state of health," *J. Power Sources*, vol. 481, Jan. 2021, Art. no. 228861.

[28] J. Yang, J. Yu, D. Tang, and J. Dai, "A closed-loop voltage prognosis for lithium-ion batteries under dynamic loads using an improved equivalent circuit model," *Microelectron. Rel.*, vols. 100–101, Sep. 2019, Art. no. 113459.

[29] X. Bian, L. Liu, J. Yan, Z. Zou, and R. Zhao, "An open circuit voltage-based model for state-of-health estimation of lithium-ion batteries: Model development and validation," *J. Power Sources*, vol. 448, Feb. 2020, Art. no. 227401.

[30] X. Lai, S. Wang, S. Ma, J. Xie, and Y. Zheng, "Parameter sensitivity analysis and simplification of equivalent circuit model for the state of charge of lithium-ion batteries," *Electrochim. Acta*, vol. 330, Jan. 2020, Art. no. 135239.

[31] J. Tian, R. Xiong, and Q. Yu, "Fractional-order model-based incremental capacity analysis for degradation state recognition of lithium-ion batteries," *IEEE Trans. Ind. Electron.*, vol. 66, no. 2, pp. 1576–1584, Feb. 2019.

[32] C. F. Zou, L. Zhang, X. Hu, Z. Wang, T. Wik, and M. Pecht, "A review of fractional-order techniques applied to lithium-ion batteries, lead-acid batteries, and supercapacitors," *J. Power Sources*, vol. 390, pp. 286–296, Jun. 2018.

[33] K. Smith and C.-Y. Wang, "Power and thermal characterization of a lithium-ion battery pack for hybrid-electric vehicles," *J. Power Sources*, vol. 160, no. 1, pp. 662–673, 2006.

[34] L. Gurjer, P. Chaudhary, and H. K. Verma, "Detailed modelling procedure for lithium-ion battery using Thevenin equivalent," in *Proc. IEEE Int. Conf. Electr., Comput. Commun. Technol. (ICECCT)*, Feb. 2019, pp. 1–6, doi: 10.1109/ICECCT.2019.8869224.

[35] Y. Cui, P. Zuo, C. Du, Y. Gao, J. Yang, X. Cheng, Y. Ma, and G. Yin, "State of health diagnosis model for lithium ion batteries based on real-time impedance and open circuit voltage parameters identification method," *Energy*, vol. 144, pp. 647–656, Feb. 2018.

[36] Z. Chen, C. C. Mi, Y. Fu, J. Xu, and X. Gong, "Online battery state of health estimation based on genetic algorithm for electric and hybrid vehicle applications," *J. Power Sources*, vol. 240, pp. 184–192, Oct. 2013.

[37] Q. Wang, Z. Wang, L. Zhang, P. Liu, and Z. Zhang, "A novel consistency evaluation method for series-connected battery systems based on real-world operation data," *IEEE Trans. Transport. Electrific.*, vol. 7, no. 2, pp. 437–451, Jun. 2021.

[38] E. B. Miftahullatif, S. Yamauchi, J. Subramanian, Y. Ikeda, and T. Kohno, "Novel state-of-health prediction method for lithium-ion batteries in battery storage system by using voltage variation at rest period after discharge," in *Proc. IEEE 4th Int. Future Energy Electron. Conf. (IFEEC)*, Nov. 2019, pp. 1–5, doi: 10.1109/IFEEC47410.2019.9015133.

[39] A. Fly and R. Chen, "Rate dependency of incremental capacity analysis (dQ/dV) as a diagnostic tool for lithium-ion batteries," *J. Energy Storage*, vol. 29, Jun. 2020, Art. no. 101329.

[40] S. Zhang, X. Guo, X. Dou, and X. Zhang, "A rapid online calculation method for state of health of lithium-ion battery based on Coulomb counting method and differential voltage analysis," *J. Power Sources*, vol. 479, Dec. 2020, Art. no. 228740.

[41] Z. Guo, X. Qiu, G. Hou, B. Y. Liaw, and C. Zhang, "State of health estimation for lithium ion batteries based on charging curves," *J. Power Sources*, vol. 249, pp. 457–462, Mar. 2014.

[42] M. Dubarry, B. Y. Liaw, M.-S. Chen, S.-S. Chyan, K.-C. Han, W.-T. Sie, and S.-H. Wu, "Identifying battery aging mechanisms in large format Li ion cells," *J. Power Sources*, vol. 196, no. 7, pp. 3420–3425, 2011.

[43] M. Dubarry, C. Truchot, and B. Y. Liaw, "Cell degradation in commercial $LiFePO_4$ cells with high-power and high-energy designs," *J. Power Sources*, vol. 258, pp. 408–419, Jul. 2014.

[44] H. Quinard, E. Redondo-Iglesias, S. Pelissier, and P. Venet, "Fast electrical characterizations of high-energy second life lithium-ion batteries for embedded and stationary applications," *Batteries*, vol. 5, no. 1, p. 33, Mar. 2019.

[45] B. Saha and K. Goebel. (2007). *Battery Data Set*. NASA Ames Research Center. Moffett Field, CA, USA. [Online]. Available: https://ti.arc.nasa.gov/project/prognostic-data-repository

[46] S. Nejad, D. T. Gladwin, and D. A. Stone, "A systematic review of lumped-parameter equivalent circuit models for real-time estimation of lithium-ion battery states," *J. Power Sources*, vol. 316, pp. 183–196, Jun. 2016.

[47] H. He, R. Xiong, and J. Fan, "Evaluation of lithium-ion battery equivalent circuit models for state of charge estimation by an experimental approach," *Energies*, vol. 4, no. 4, pp. 582–598, Dec. 2011.

[48] T. Feng, L. Yang, X. Zhao, H. Zhang, and J. Qiang, "Online identification of lithium-ion battery parameters based on an improved equivalent-circuit model and its implementation on battery state-of-power prediction," *J. Power Sources*, vol. 281, pp. 192–203, May 2015.

[49] F. Leng, C. M. Tan, and M. Pecht, "Effect of temperature on the aging rate of Li ion battery operating above room temperature," *Sci. Rep.*, vol. 5, no. 1, pp. 1–12, Oct. 2015.

[50] J. Zhang, P. Wang, Y. Liu, and Z. Cheng, "Variable-order equivalent circuit modeling and state of charge estimation of lithium-ion battery based on electrochemical impedance spectroscopy," *Energies*, vol. 14, no. 3, p. 769, Feb. 2021.

[51] N. Somakettarin and T. Funaki, "An experimental study on modeling of transient response and parameters identification for Mn-type Li-ion battery with temperature dependency," in *Proc. Int. Conf. Renew. Energy Res. Appl. (ICRERA)*, Oct. 2014, pp. 804–809.

SHEHLA AMIR received the B.Sc. degree in electrical engineering from the Lahore University of Management Sciences (LUMS), Lahore, Pakistan. She is currently a Research Assistant at the Department of Electrical Engineering, LUMS. Her research interests include wireless sensing, wireless communications, and battery storage systems.

MONEEBA GULZAR received the B.S. degree in electrical engineering from the Lahore University of Management Sciences (LUMS), Lahore, Pakistan. She is currently a Teaching Assistant at the Electrical Engineering Department, LUMS. Her research interests include power electronics, battery storage systems, and electric vehicles.

MUHAMMAD O. TARAR received the B.Sc. degree in electrical engineering from the University of Engineering and Technology Lahore, Pakistan, and the M.S. degree in electrical engineering from the Lahore University of Management Sciences (LUMS), Lahore, Pakistan, in 2019, where he is currently pursuing the Ph.D. degree with the Department of Electrical Engineering.

His research interests include battery storage systems, electric vehicles, and reliability study of batteries especially Li-ion.

IJAZ H. NAQVI (Member, IEEE) received the B.Sc. degree in electrical engineering from the University of Engineering and Technology Lahore, Pakistan, in 2003, the master's degree in radio communications from SUPELEC Paris, France, in 2006, and the Ph.D. degree in electronics and telecommunications from the IETR-INSA Rennes, France, in 2009.

He is currently an Associate Professor at the School of Science and Engineering, Lahore University of Management Sciences (LUMS), Lahore, Pakistan. He has got several years of research experience in the wireless communications and wireless sensor networks. He also works in the area of reliability engineering investigating degradation and ageing of electronics specially Li-ion batteries. He has published several refereed papers in international journals and peer-reviewed international conferences. His current research interests include 5G networks and beyond, including system level aspects in wireless networks, millimeter wave wireless systems for 5G and 6G telecommunication, and multi-antenna radar systems for civilian applications.

NAUMAN A. ZAFFAR (Member, IEEE) received the B.S. and M.S. degrees in electrical engineering from the University of Pennsylvania, in 1990 and 1991, respectively.

He is currently an Associate Professor and the Director of the Energy and Power Systems Research Cluster, Department of Electrical Engineering, Syed Babar Ali School of Science and Engineering, Lahore University of Management Sciences, Lahore, Pakistan. His primary research focus is on harnessing and efficient utilization of energy from available sources, such as solar PV, solar thermal, wind, and hydrokinetics to enable energy independent, integrated, smart grid communities, and development of electric vehicles value chains. He has been actively engaged in arranging and delivering national workshops in core areas of circuits, electronics, power electronics, and design of magnetics. His research interests include work on smarts for existing grids and new grid architectures, electricity markets, power electronic converters for integration of renewable energy resources, electrical drives, battery storage systems, and electrical vehicles.

MICHAEL G. PECHT (Life Fellow, IEEE) received the B.S. degree in physics, the M.S. degree in electrical engineering, and the M.S. and Ph.D. degrees in engineering mechanics from the University of Wisconsin–Madison.

He is currently the Founder and the Director of the Center for Advanced Life Cycle Engineering, University of Maryland, which is funded by over 150 of the world's leading electronics companies at over U.S. 6 M/year. He is also a Chair Professor of mechanical engineering and a Professor of applied mathematics with the University of Maryland. He is a fellow of ASME, SAE, and IMAPS. He received the NSF Innovation Award in 2009 and the National Defense Industries Association Award. In 2015, he received the IEEE Components, Packaging, and Manufacturing Award for Visionary Leadership in the development of physics-of-failure-based and prognostics-based approaches to electronic packaging reliability. He received the Distinguished Chinese Academy of Sciences President's International Fellowship. In 2013, he received the University of Wisconsin–Madison's College of Engineering Distinguished Achievement Award. In 2011, he received the University of Maryland's Innovation Award for his new concepts in risk management. In 2010, he received the IEEE Exceptional Technical Achievement Award for his innovations in the area of prognostics and systems health management. In 2008, he was a recipient of the highest reliability honor, the IEEE Reliability Society's Lifetime Achievement Award. He is a World-Renowned Expert in strategic planning, design, test, and risk assessment of information systems. He is the Editor-in-Chief of IEEE Access. He served as a Chief Editor of the IEEE Transactions on Reliability for a period of nine years and the *Microelectronics Reliability* for a period of 16 years. He has also served on three NAS studies, two U.S. Congressional investigations in automotive safety, and as an Expert for the FDA. He is also a Professional Engineer.